# Technical ~~n~~Note: A revised numerical model for ~~W~~wellbore water volume computation in a confined aquifer~~of~~ during chemicals ~~tracer test in numerical modelling~~transport in a wellbore-aquifer system ~~in a confined aquifer~~

Yiqun Gan[a, b] and Quanrong Wang[a, b*]

[a]School of Environmental Studies, China University of Geosciences, Wuhan, Hubei 430074, PR China

[b]Key Laboratory of Groundwater Quality and Health of Ministry of Education, China University of Geosciences, Wuhan 430074, China

***Correspondence to***: Quanrong Wang (wangqr@cug.edu.cn)

## Abstract.

Wellbore is proven to be the only effective way to deliver chemicals into a target aquifer during a tracer test or aquifer remediation. The volume of original water in the operational well is a critical parameter, affecting the concentration of injected tracers or chemicals in the wellbore in the early stages. We found that the calculation of the wellbore water volume by previous numerical methods was correct when the wellbore penetrates an unconfined aquifer, but incorrect when the wellbore penetrates a confined aquifer, further resulting in errors in describing the solute transport of injected chemicals in confined aquifers, such as MODFLOW/MT3DMS, FEFFLOW, and so on. Such errors caused by MODFLOW/MT3DMS and FEFFLOW increased with increasing wellbore water volume. This was because the groundwater in both wellbore and aquifer was assumed to be confined, where the water level was higher than the aquifer's top elevation, and the groundwater thickness was assumed to be equal to the aquifer thickness. Actually, when the wellbore penetrated a confined aquifer, the groundwater was only confined in the aquifer, while it was unconfined in the wellbore. In this study, the solute transport model is revised based on the mass balance in a well-aquifer system, with special attention given to the wellbore water volume. The accuracy of the new model was tested against benchmark analytical solutions. The revised model could increase the accuracy of reactive transport modeling in aquifer remediation through the wellbore.

**Keywords:** Wellbore; Radial dispersion; Finite-difference scheme; Mixing processes

## 1 Introduction

Wellbore is ~~only~~ an effective way to deliver chemicals into a target aquifer for the purpose of parameter estimation in a tracer test or aquifer remediation~~used to obtain the physical and chemical parameters of an actual confined aquifer during aquifer remediation or tracer test~~ (Anderson et al., 2015; El-Kadi, 1988). As groundwater flow is complex in the subsurface, ~~how much chemicals should be~~ the amount of chemicals to be delivered and the area of final concentration ~~delivered or where do they move~~ after entering ~~into~~ the aquifers have to be evaluated by mathematical models~~For instance, the chemicals are injected or extracted through it during the *in-situ* tracer test, and then the parameters, like dispersivity, chemical reaction rate, etc, are estimated by the mathematical models through best fitting the time series concentration observed during tracer test~~. Therefore, the robustness of the mathematical models of ~~tracer test~~solute transport is critical for accuracy and interpretation. ~~for the accuracy of parameter estimation~~.

According to the treatment of solute transport in wellbore, the mathematical models could be classified into two types, which will be reviewed in Section 2. The first type of mathematical models consider the wellbore as an inner boundary condition of reactive transport in the aquifer (named the IBC model), and they are preferred by the analytical solutions, while in the second type of mathematical models, the well is treated as a source or sink (named as the SS model), and they are preferred by the numerical solutions due to the complexity of hydrogeological conditions (like heterogeneity and transiency of flow field).

The SS models of tracer test are composed of two parts: solute transport in the wellbore and the aquifer. In the confined aquifer, the wellbore is open to the air, hence making it unconfined. After a careful literature review, we found that previous numerical solutions of two-dimensional (2D) and three-dimensional (3D) SS models of tracer test in the Cartesian coordinate system did not properly deal with the mixing processes between the original water and tracers entering into the operational wellbore in a confined aquifer. The objectives of this study include~~:~~ the revisit of the treatment of wellbore storage in mathematical models of reactive transport in a wellbore-aquifer system, the revision of ~~–~~numerical solution of the SS model describing the mixing processes between solutes in the wellbore during the ~~reactive~~ solute transport, and the validation of the revised model.

## 2. Review of mathematical models of solute transport in wellbore-aquifer system

### *2.1 The IBC model of solute transport*

When the wellbore is considered as an inner boundary condition, the wellbore-aquifer system reduces the aquifer system, as the concentration variation of solute in the wellbore is not included in the governing equation (Veling, 2012; Wang and Zhan, 2013), e.g.,

$$\frac{\partial(\theta C^k)}{\partial t} = L_{DSP}(C^k)+L_{ADV}(C^k)+L_{SSM}(C^k) + L_{RCT}(\theta C^k),\ t > 0, \quad (1)$$

$$C^k(r,z,t)|_{r=r_w} = f(z,t),\ t > 0, \quad (2a)$$

$$\text{or } \left[v_r C^k(r,z,t) - \alpha_r|v_r|\frac{\partial C^k(r,z,t)}{\partial r}\right]\Big|_{r=r_w} = v_r f(z,t),\ t > 0, \quad (2b)$$

where $C^k$ is dissolved concentration of species $k$ [ML$^{-3}$]; $k$ is a positive integral to account for the number of species [dimensionless]; $t$ is time [T]; $r$ is radial distance from the wellbore [L]; $z$ is vertical distance;

$\theta$ is porosity of the porous medium [dimensionless]; $r_w$ is wellbore radius [L]; $\alpha_r$ and $v_r$ are radial dispersivity [$L^2T^{-1}$] and radial flow velocity [$LT^{-1}$], respectively; $L_{DSP}(\cdot)$, $L_{ADV}(\cdot)$, $L_{SSM}(\cdot)$, and $L_{RCT}(\cdot)$ are operators for dispersion, advection, other sink/sources excluding the discharge/recharge in the wellbore, and chemical reaction terms, respectively; $f(t)$ represents the concentration variations of solute in the wellbore, which is a function of time. Eq. (1) is the multi-species governing equation of reactive transport. Eqs. (2a) - (2b) are the inner boundary conditions, representing the resident concentration continuity and the flux concentration continuity at the well-aquifer interface, respectively, while Eq. (2b) is recommended since it could keep mass balance for solute transport in the aquifer. The difference between them could be seen in Schwartz et al. (1999) and Novakowski (1992).

This type of models is generally established in the radial coordinate system, such as Wang and Zhan (2013). This is because the flow field is radial when only one well exists and the regional flow (or ambient flow) is negligibly small. The advantage of the radial coordinate system is that it could simplify the mathematical models from two dimensions into one dimension (Chen, 1985; Chen et al., 2012; Novakowski, 1992) or from three dimensions into two dimensions (Huang et al. 2010; Chen, 2010; Chen et al., 2011), for which elegant analytical models may be developed. As for the 2D radial transport, the operators of $L_{DSP}(\cdot)$, $L_{ADV}(\cdot)$, $L_{SSM}(\cdot)$, and $L_{RCT}(\cdot)$ are

$$L_{DSP}(C^k) = \frac{1}{r}\frac{\partial}{\partial r}\left(rD_{rr}\frac{\partial C^k}{\partial r} + rD_{rz}\frac{\partial C^k}{\partial z}\right) + \frac{\partial}{\partial z}\left(D_{zr}\frac{\partial C^k}{\partial z} + D_{zz}\frac{\partial C^k}{\partial z}\right), \quad (3)$$

$$L_{ADV}(C^k) = v_r\frac{\partial C^k}{\partial r} + v_z\frac{\partial C^k}{\partial z}, \quad (4)$$

$$L_{SSM}(C^k) = q_s C^k, \quad (5)$$

$$L_{RCT}(\theta C^k) = \sum R_n, \quad (6)$$

where $D_{rr}$, $D_{rz}$, $D_{zr}$ and $D_{zz}$ are the four components of the dispersion coefficient tensor [$L^2T^{-1}$], respectively; $\sum R_n$ is chemical reaction term [$ML^{-3}T^{-1}$]; $q_s$ is the volumetric flow rate per unit volume which does not include the pumpage of the wellbore [$T^{-1}$]; $v_z$ is vertical flow [$LT^{-1}$].

However, these types of models have two shortcomings. Firstly, the flow field may ~~be~~ not be radial in realistic aquifer settings, for instance, when more than one well exists or the regional flow could be ignored. Secondly, Eq. (2a) or Eq. (2b) is used to describe the transport at the well screen, and the concentration in the wellbore is required, e.g. $f(z,t)$, which may be unknown in reality. For ~~the~~ simplicity, many studies have assumed that $f(z,t)$ equal~~sed~~ the concentration of the injected solute inside the wellbore (Chen, 1985; Chen, 2010; Phanikumar and McGuire, 2010; Yeh and Chang, 2013a):

$$f(z,t) = C_{inj}^{k}, \tag{7}$$

where $C_{inj}^{k}$ is the concentration of species $k$ in the injected solute [$ML^{-3}$]. ~~It~~ This is not true, since Eq. (7) does not consider the mixing processes between original water and tracers entering into the operational wellbore, and it overestimates the values of concentration in the wellbore. Novakowski (1992) presented a well model considering the wellbore storage for different scenarios based on the mass balance principle, while the flow field was assumed to be in steady state, and the mixing processes were assumed to be instantaneously completed.

### *2.2 The SS model of solute transport*

Because of the limitations ~~included in~~ of the IBC model, the popular way is to ~~take~~ consider the wellbore as a source/sink term in the governing equation of reactive transport in the numerical modeling. The governing equation of multi-species reactive transport in the wellbore-aquifer system becomes (Konikow and Grove, 1977; Zheng and Wang, 1999):

$$\frac{\partial(\theta C^k)}{\partial t} = L_{DSP}(C^k)+L_{ADV}(C^k)+L_{SSM}(C^k)+L_{RCT}(\theta C^k) + q_w C_w^k,\ t > 0, \quad (8)$$

where $q_w$ is volumetric flow rate per unit volume of aquifer [$T^{-1}$], and it is positive for injection (when the well acts as a source), and negative for extraction (when the well acts as a sink); $C_w^k$ is the concentration of species $k$ [$ML^{-3}$], and it is equal to $C^k$ in the case of extraction ($q_s$<0); the operators of $L_{DSP}(\cdot)$ and $L_{ADV}(\cdot)$ are different from ones defined in Eq. (1), for instance,

$$L_{DSP}(C^k) = \frac{\partial}{\partial x_i}\left(\theta D_{ij}\frac{\partial C^k}{\partial x_j}\right), \quad (9)$$

$$L_{ADV}(C^k) = \frac{\partial}{\partial x_i}(\theta v_i C^k), \quad (10)$$

where $x_i$ is distance [L] along the respective Cartesian coordinate axis, $i$ =1, 2, and 3, representing the $x$, $y$, and $z$ axes, respectively; $D_{ij}$ is hydrodynamic dispersion coefficient tensor [$L^2T^{-1}$]; $v_i$ is flow velocity. The definitions of $L_{SSM}(\cdot)$ and $L_{RCT}(\cdot)$ are the same as the ones in Eq. (1). The boundary of Eq. (4) is set far away from the well, where the concentration is equal to the background value.

Different from the first approach in Section 2.1, only the values of $q_w$ and $C_w^k$ are required, which are generally available. Eqs. (8) - (10) have been widely employed for solute transport modeling in many software packages, like MODFLOW/MT3DMS (Zheng and Wang, 1999), FEFLOW (Trefry and Muffels, 2007), TOUGH2 (Pruess et al., 2011), etc.

### *2.3 Groundwater flow model of tracer test in confined aquifer*

Solute transport in ~~the~~ aquifers is mainly controlled by groundwater flow, like dispersion, advection, and reactions, and therefore the mathematical models of groundwater flow have to be solved to obtain the flow velocity or the hydraulic head before solving the models of solute transport. For instance, in the

software package ~~of~~ MODFLOW/MT3DMS, the modeling of groundwater flow by MODFLOW is run first~~ly~~ to produce the spatiotemporal flow ~~filed~~ field for modeling solute transport by MT3DMS.

## 3. Errors of the previous numerical models

### ~~3.1 Errors of the previous finite-difference scheme of the SS models~~

The MODFLOW/MT3DMS package and the FEFLOW package are based on the finite difference method and the finite element method, respectively. As MODFLOW/MT3DMS is ~~a~~ free and open source, it could be easily revised~~ easily~~, and we mainly analyze the errors of this numerical model. The finite-difference scheme of the MODFLOW/MT3DMS model of tracer test in confined aquifers in the wellbore-aquifer system is (Konikow and Grove, 1977; Zheng and Wang, 1999):

$$MA_{Cell} = NMF_x + NMF_y + NMF_z + NMFSS_{Cell} + NMFR_{Cell}, \quad (11)$$

where

$$NMF_x = -\frac{\partial}{\partial x}(C^k \theta v_x^* \Delta y \Delta z)\Delta x, \quad (12a)$$

$$NMF_y = -\frac{\partial}{\partial y}\left(C^k \theta v_y^* \Delta x \Delta z\right)\Delta y, \quad (12b)$$

$$NMF_z = -\frac{\partial}{\partial z}(C^k \theta v_z^* \Delta x \Delta y)\Delta z, \quad (12c)$$

$$NMFSS_{Cell} = W_s C_s^k \Delta x \Delta y \Delta z, \quad (12d)$$

$$NMFR_{Cell} = \theta \Delta x \Delta y \Delta z \sum R_k, \quad (12e)$$

$$MA_{Cell} = \frac{\partial}{\partial t}(C^k \theta \Delta x \Delta y \Delta z), \quad (12f)$$

where $v_x^*$, $v_y^*$, and $v_z^*$ are instantaneous mass velocities [$LT^{-1}$] along the $x$, $y$, and $z$ axes, respectively; $W_s$ is volumetric flux per volume of porous medium [$T^{-1}$]; $C_s^k$ is the concentration [$ML^{-3}$] of the solute in the source or sink fluid; $\Delta x$, $\Delta y$, and $\Delta z$ are the dimensions [L] of cell along the $x$, $y$, and $z$ axes, respectively; $MA$ is mass accumulation rate [$MT^{-1}$]; $NMF$ is net mass flux [$MT^{-1}$]; $NMFSS$ is net mass flux by source and sink [$MT^{-1}$]; $NMFR$ is net mass flux by reactions [$MT^{-1}$]. When $\Delta x = \Delta y$ and $\Delta x \Delta y = \pi r_w^2$ in the wellbore cell, $W_s$ is injection or extraction rate per volume, and $C_s^k$ is the concentration of the injected or extracted solute.

Eqs. (11) - (12) are used in the WELL package of MT3DMS for modeling reactive transport in the wellbore-aquifer system, which is suitable for the one-cell wellbore model, not for the multi-node well (MNW) model. The MNW model refers to a case when the wellbore is vertically discretized into several cells (e.g., Cell 1, Cell 2, Cell 3, and Cell 4, as shown in Figure 1). In the one-cell wellbore model, the intra-borehole flow is ignored. As for the MNW model, the intra-borehole flow is considered, and there is a special package ~~was~~ developed for both groundwater flow and solute transport based on MODFLOW/MT3DMS, named the MNW package (Konikow and Hornberger, 2006; Konikow et al., 2009).

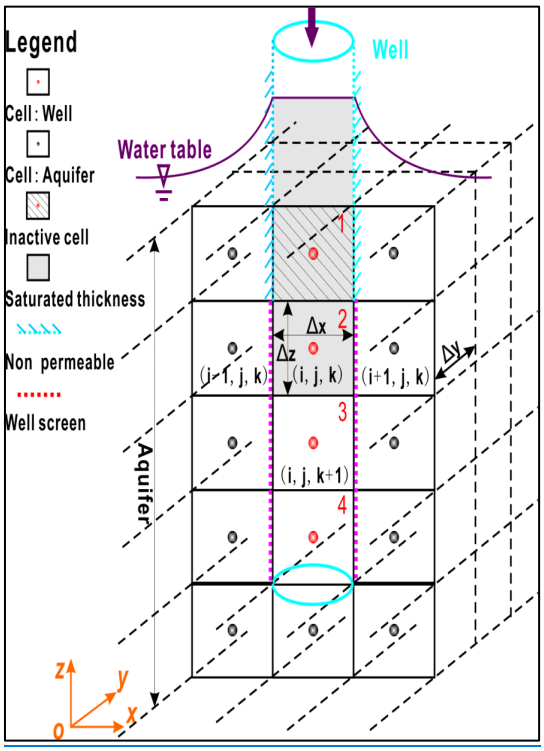


**Figure 1.** Schematic diagram of the grid system in a numerical simulation of a partially penetrating well. Black lines represent the discretization of the aquifer including the wellbore in the aquifer (e.g. Cell 1, Cell 2, Cell 3, and Cell 4). The part of the wellbore located above the aquifer is not included in the grid system.

Eqs. (12a) - (12f) demonstrate that the weaknesses of the second type of models ~~s~~ ~~is~~ are that the wellbore is treated ~~s~~ as a part of the aquifer, resulting in the following two problems:~~.~~ Firstly, the porosity of the wellbore is unity, but it is assumed to be the same as the porosity of the surrounding aquifer. Secondly, the term ~~of~~ $\theta\Delta x\Delta y\Delta z$ represents the volume of ~~the~~ water in the cells of the grid system in Figure 1, regardless of aquifer and wellbore~~.~~;~~ It~~ ~~is~~ it remains constant. Actually, the aquifer cells are different from the wellbore cells in bearing ~~the~~ groundwater. In the confined aquifer cells, the volume of water is not affected by the variation ~~of~~ in hydraulic head; however, in the wellbore, the volume of water directly changes with the variation ~~of~~ in water level.

To test the effect of assumptions included in MODFLOW/MT3DMS and FEFFLOW on solute transport in a wellbore-aquifer system, we employ a proven analytical solution that will ~~be desirable to~~ serve as the benchmark of comparison. Unfortunately, it seems not to be easy to derive a general-purpose analytical solution that can accommodate many realistic field conditions, such as flow transiency, etc. It is also necessary to test the new model with the analytical solution considering the actual well construction, such as the skin effect. However, the available analytical solutions ~~of~~ to the two-region model have not considered ~~the~~ wellbore storage. For instance, Chen et al. (2012) assumed that $f(z,t)$ in Eq. (2a) was constant and independent of location and time, and was equal to the concentration of the injected solute. Therefore, we will employ the analytical solution of an injection test by Novakowski (1992), who considered ~~the~~ wellbore storage.

Figures 2a and 2b show the comparison of the breakthrough curves (BTCs) by the analytical and numerical methods in the wellbore, where the vertical axis represents the relative (or normalized) concentration $C/C_0$, and $C_0$ is the constant concentration of the injected solute. The legend of "ANA" represents the analytical solutions by Novakowski (1992). The parameters used in this case are as follows: The aquifer dimensions are 100 m$\times$ 100 m $\times$ 6 m; the horizontal hydraulic conductivity is 10 m/day; the horizontal anisotropy is 1.0, where the horizontal anisotropy is the ratio between the two horizontal principal components of the hydraulic conductivity; the injection flow rate is 20 $m^3$/day; the porosity is 0.3; the longitudinal dispersivity is 0.5 m; the ratio of horizontal transverse dispersivity to longitudinal dispersivity is 0.1; the ratio of vertical transverse dispersivity to longitudinal dispersivity is 0.01. As the well radius is always constant, three sets of initial conditions of the hydraulic head are employed to test the influence of water level on the wellbore storage: $h_0$ =6 m, $h_0$ =30 m, and $h_0$ =60 m. A greater initial

head implies a greater water level in the wellbore. Since the depth of wellbore might be greater than 100 m, sometime 1000 m for a deep confined aquifer, the maximum value of 60 m for $h_0$ is not unusual for the initial hydraulic head. As the flow is assumed to be steady state, the information of the specific yield and the specific storage is not needed. The spatial discretization is $\Delta x = 0.4$ m, $\Delta y = 0.4$ m, and $\Delta z$=6 m. The aquifer is vertically discretized into one layer. This is because the flow direction is radially horizontal for a well fully penetrating a homogeneous aquifer. The steady-state drawdown in the wellbore is set as -0.346 m for all cases.

A point to note is that wellbore is a cylinder in the analytical solution, while it is approximated as a cuboid in the numerical solution by MODFLOW/MT3DMS. To ensure the same water volume used in both analytical and numerical solutions, the well radius ($r_w$) of the analytical solution is calculated by the following equation:

$$r_w = \sqrt{\frac{\Delta x \Delta y}{\pi}}. \quad (13\text{~~16~~})$$

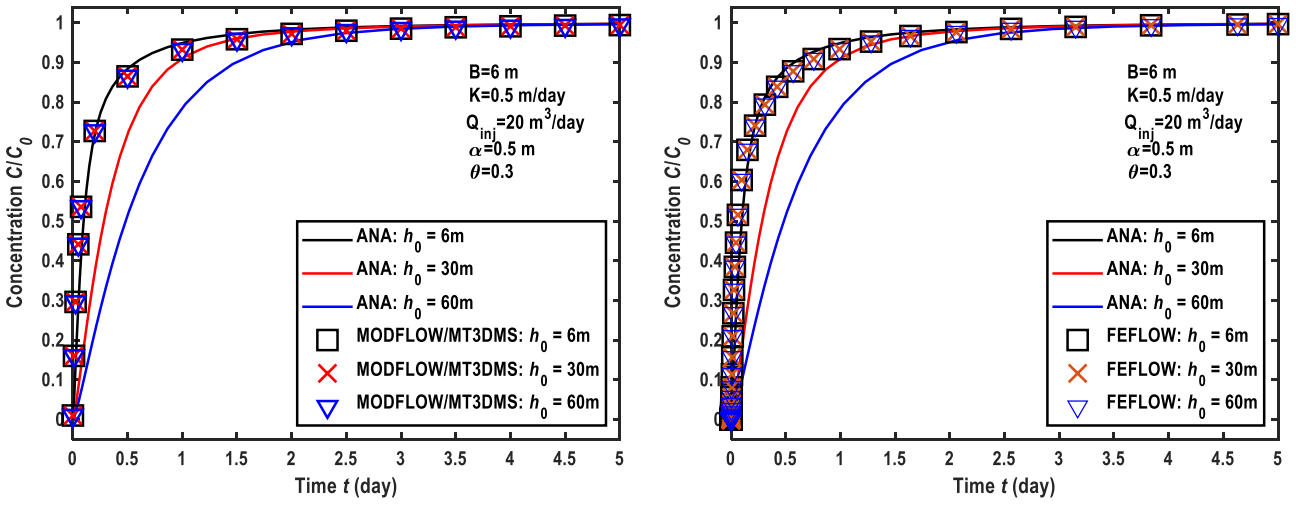


**Figure 2.** Comparison between BTCs based on analytical and numerical methods in the wellbore under steady state flow conditions. ANA: Analytical solutions.

Figures 2a and 2b shows that the numerical solution by previous MODFLOW/MT3DMS code and FEFLOW is independent of the water level in the wellbore, which is close to the analytical solution when the initial water level inside the wellbore is 6 m (the same as the aquifer thickness). However, when the initial water level inside the wellbore is substantially different from the aquifer thickness of 6 m, considerable discrepancies can be seen between the analytical and numerical solutions. These two figures demonstrate that the previous models of Eqs. (8) - (12) may cause significant errors in describing solute transport around a wellbore when the initial water level inside the wellbore is considerably different from the aquifer thickness.

~~The finite-difference scheme of the SS model of tracer test in confined aquifer in the wellbore-aquifer system is (Konikow and Grove, 1977; Zheng and Wang, 1999):~~

~~In the early stage of pumping or extracting phase, the volume of water in the wellbore is critical for the wellbore storage of solute transport. Greater volume results in smaller concentration of solute in the wellbore, due to the mixing processes between the original water in the wellbore and water entering the wellbore or leaving the wellbore.~~

## ~~3.2~~4. Revised finite-difference scheme of the SS models

In this study, Eqs. (8) - (12) are called the “previous models” hereinafter and will be revised by considering the water level variation in a wellbore. Including the wellbore cells in the numerical

simulation of flow in a well-aquifer system imposes new challenges. For instance, the simulated aquifer is confined, whereas the simulated open wellbore is unconfined. The wellbore may include permeable screen sections and impermeable casings, as shown in Figure 1. Therefore, how to treat the wellbore cells in the numerical models needs to be clarified.

Figure 1 shows the grid system for the general case in the numerical simulation. The well is discretized into several cells, e.g., Cell 1, Cell 2, Cell 3, and Cell 4, and such a well is named as a multi-node well. When the well is discretized into one cell, a multi-node well reduces to a one-cell well. Cell 2, Cell 3, and Cell 4 in Figure 1 represent the permeable screen, which could be treated as point sources/sinks in the model. Cell 1 in Figure 1 represents the impermeable casing, which is the upper most cell above the screen inside wellbore.

As for Cell 1, the lateral boundary is impermeable, which implies that it can only exchange water with Cell 2. Therefore, Cell 1, wellbore above Cell 1, and Cell 2 could be combined into one cell, e.g., a revised Cell 2. The volume of water in this revised Cell 2 is the summation of water in Cell 1, water in wellbore above Cell 1, and water in the original Cell 2. Namely, the volume of water in this revised cell is $\Delta x \Delta y B_{Cell2,w}$, where $B_{Cell2,w} = h_w - z_{Cell2,bot}$; $z_{Cell2,bot}$ is the vertical coordinate of the bottom of Cell 2; $h_w$ is water level of the wellbore. For a confined aquifer, one has $B_{Cell2,w} > \Delta z_{Cell2,w}$, where $\Delta z_{Cell2,w}$ represents the vertical dimension of Cell 2. The validity of such treatment will be investigated in Section 4.2.

Therefore, the mass balance for the revised Cell 2 should be

$$MA_{Cell2} = \frac{\partial}{\partial t}\left(C^k \Delta x \Delta y B_{Cell2,w}\right), \quad (14\sout{13})$$

and Eq. (12d) becomes

$$NMFSS_{Cell} = W_s C_s^k \Delta x \Delta y B_{Cell2,w}. \quad (15\sout{14})$$

Since the porosity of the revised Cell 2 is unity, $NMFR_{Cell}$ in Eq. (11) becomes

$$NMFR_{Cell} = \Delta x \Delta y B_{Cell2,w} \sum R_k. \quad (16\sout{15})$$

The other terms of the revised Cell 2 in Eq. (11) are the same as their counterparts in Eqs. (12a) - (12f). As for other wellbore cells, the mass balance equations are the same as ones in Eq. (11), except that porosity is set as unity. As for aquifer cells, the mass balance equations are the same as Eq. (11).

Similar to MODFLOW/MT3DMS, the finite-difference method will be employed to solve Eq. (8). The code of MT3DMS will be revised to accommodate the above special treatments of the wellbore cells (particularly the revised Cell 2 in Figure 2) in this study. The flow field is computed by MODFLOW. The changes of the original MT3DMS code are explained in Sections 1 and 2 of Supplementary Materials.

As for a one-cell wellbore (when the well is discretized into a cell), solute transport in the well could be similarly treated by equations used in the revised Cell 2.

### ~~*3.3 Transport models in the wellbore*~~

In actual applications, the flow field is complex for either an injection well or an extraction well, as shown in the laboratory-controlled experiment of Wang et al. (2018), due to turbulent flow caused by the injection/extraction apparatus (usually a pipe) with a smaller diameter than that of the wellbore itself. Different from transport in porous media, the mechanism of solute transport in the wellbore is similar to transport in surface water bodies (e.g. river). Therefore, diffusion effect and advection are considered for solute transport in the wellbore, while mechanical dispersion is absent (because there is no porous media

inside the wellbore). In this study, the MNW model (Konikow and Hornberger, 2006) is used to describe the groundwater flow and solute transport in the wellbore, which is based on MODFLOW/MT3DMS.

## 45. Accuracy of the revised finite-difference scheme of the SS models

Figures 2a and 2b 3 shows the comparison of the breakthrough curves (BTCs) by the analytical and revised numerical methods in the wellbore, where the vertical axis represents the relative (or normalized) concentration $C/C_0$, and $C_0$ is the constant concentration of the injected solute. The legend of "ANA" represents the analytical solutions. The parameters used in this case are as follows: The aquifer dimensions are 100 m× 100 m × 6 m; the horizontal hydraulic conductivity is 10 m/day; the horizontal anisotropy is 1.0, where the horizontal anisotropy is the ratio between the two horizontal principal components of the hydraulic conductivity; the injection flow rate is 20 $m^3$/day; the porosity is 0.3; the longitudinal dispersivity is 0.5 m; the ratio of horizontal transverse dispersivity to longitudinal dispersivity is 0.1; the ratio of vertical transverse dispersivity to longitudinal dispersivity is 0.01. As the well radius is always constant, three sets of initial conditions of the hydraulic head are employed to test the influence of water level on the wellbore storage: $h_0$ =6 m, $h_0$ =30 m, and $h_0$ =60 m. A greater initial head implies a greater water level in the wellbore. Since the depth of wellbore might be greater than 100 m, sometime 1000 m for a deep confined aquifer, the maximum value of 60 m for $h_0$ is not unusual for the initial hydraulic head. As the flow is assumed to be steady state, the information of the specific yield and the specific storage is not needed. The spatial discretization is $\Delta x = 0.4$ m, $\Delta y = 0.4$ m, and $\Delta z$=6 m. The aquifer is vertically discretized into one layer. This is because the flow direction is radially

horizontal for a well fully penetrating a homogeneous aquifer. The steady-state drawdown in the wellbore is set as -0.346 m for all cases. the same as ones used in Figure 2.

A point to note is that wellbore is a cylinder in the analytical solution, while it is approximated as a cuboid in the numerical solution by MODFLOW/MT3DMS. To ensure the same water volume used in both analytical and numerical solutions, the well radius ($r_w$) of the analytical solution is calculated by the following equation:

$$r_w = \sqrt{\frac{\Delta x \Delta y}{\pi}}. \quad (16)$$

Figure 2a shows that the numerical solution by previous MT3DMS code is independent of the water level in the wellbore, which is close to the analytical solution when the initial water level inside the wellbore is 6 m (the same as the aquifer thickness). However, when the initial water level inside the wellbore is substantially different from the aquifer thickness of 6 m, considerable discrepancies can be seen between the analytical and numerical solutions. This figure demonstrates that the previous models of Eqs. (8) - (12) may cause significant errors in describing solute transport around a wellbore when the initial water level inside the wellbore is considerably different from the aquifer thickness. Figure 2b shows the comparison between the analytical solution and numerical solution by the revised MT3DMS code of this study, and they match well with each other, with some minor discrepancies (but noticeable). Such minor discrepancies may be caused by two factors. First, the vertical surface area of the screen in the analytical solution (cylinder) is different from that in the numerical solution (cuboid) when the volume of the cuboid well is equal to the volume of the cylinder well. For instance, based on the setting of this study ($r_w$= 0.226 m, $B$ =6 m, $\Delta x$ = 0.4 m), the surface area of a cylinder is $2\pi r_w B$=8.51 m$^2$, while the vertical

~~surface area of a cuboid is $4\Delta xB$=9.60 m$^2$. Such a difference in surface area of the screen may generate a minor discrepancy between the analytical and numerical solutions. Second, numerical errors (like numerical dispersion) may not be completely eliminated in the finite-difference solution.~~

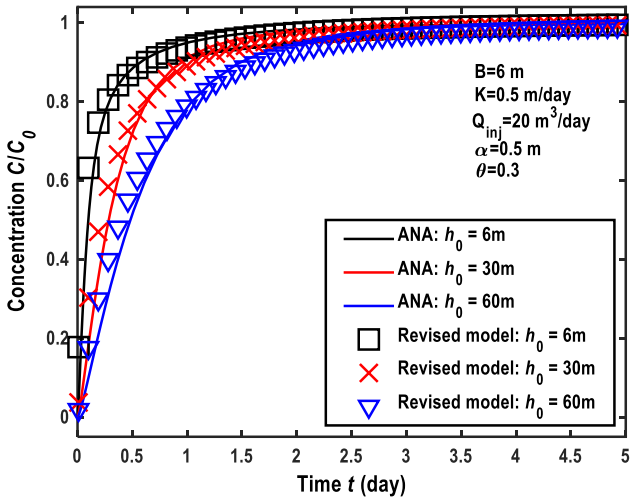


**Figure 3.** Comparison between BTCs based on analytical and revised numerical methods in the wellbore under steady state flow conditions. ANA: Analytical solutions.

This figure shows the comparison between the analytical solution and the numerical solution by the revised MT3DMS code of this study, and they match well with each other, with some minor discrepancies (but noticeable). Such minor discrepancies may be caused by two factors. First, the vertical surface area of the screen in the analytical solution (cylinder) is different from that in the numerical solution (cuboid) when the volume of the cuboid well is equal to the volume of the cylinder well. For instance, based on the setting of this study ($r_w$= 0.226 m, $B$ =6 m, $\Delta x$ = 0.4 m), the surface area of a cylinder is $2\pi r_w B$=8.51 m$^2$, while the vertical surface area of a cuboid is $4\Delta xB$=9.60 m$^2$. Such a difference in surface area of the screen may generate a minor discrepancy between the analytical and numerical solutions. Second,

numerical errors (like numerical dispersion) may not be completely eliminated in the finite-difference solution.

In addition, it is desirable to test the new models using an extraction well test. However, the analytical solution for such a case is not available if the wellbore storage must be taken into consideration. This is an open research problem that will be investigated in the near future.

## ~~5. Discussions~~

~~In aquifer remediation practices, both injection and extraction wells have been widely employed (Anderson et al., 2015; El-Kadi, 1988). Although the influence of the wellbore storage has been investigated for an injection well test case in Section 4, an important assumption should not be overlooked: the flow is under steady-state condition, which might not always be satisfied in actual applications. In this section, the wellbore storage of solute transport around both injection and extraction wells under transient flow condition will be investigated to see how the flow transiency will affect the results obtained from the steady-state assumption.~~

### ~~*5.1 The injection test in a homogeneous aquifer*~~

~~Figure 3 shows the comparison of BTCs between the previous models of Eqs. (8) – (12) and revised models of this study Eqs. (13) – (15) at different vertical locations. The value of specific storage is 0.00001 $m^{-1}$, and the initial water table is 60 m. The parameters used are the same with ones in Figure 2. The legend of "in aquifer" represents the case that the observed BTCs is 3 m away from the wellbore.~~

This figure demonstrates that the values of BTCs computed by the previous models are smaller than those by the new model, and the difference between them is obvious in both aquifer and wellbore. It demonstrates that errors caused by Eqs. (8) - (12) are not negligible for the case with an injection well.

### *5.2 The extraction test in a homogeneous aquifer*

Figure 4 shows the comparison of BTCs between the previous models and the revised models of this study around an extraction well. The legend of "in aquifer" represents the case that the observed BTCs is 3 m away from the wellbore. The flow rate is -20 $m^3$/day where negative sign represents extraction. The initial solute plume is a cuboid. Horizontally, the extraction well is located at the center of the plume cuboid, and the side faces of the plume are 5 m away from the well center. The other parameters are the same with ones in Figure 3. This figure shows that BTCs computed by the new model are above ones by the previous model, due to the wellbore storage considered in the new model. The difference of BTCs between them is obvious in the wellbore, but not in the aquifer. One may find that the wellbore storage is generally not significant for solute transport in the aquifer at locations not too close to the wellbore, e.g. 3 m in this study. The reason is that the solute mainly moves toward the well, due to the convergent flow field, and the wellbore storage on the aquifer could be ignored.

Therefore, this figure demonstrates that the errors caused by Eqs. (8) - (12) are generally negligible for reactive transport in the aquifer at locations not too close to the wellbore (such as 3 m), but those errors are not negligible for the wellbore.

### *5.3 The injection test in a heterogeneous aquifer*

Generally, the aquifer homogeneity is a simplification of reality. In this section, the aquifer is assumed to be vertically heterogeneous. The vertical heterogeneity is manifested in multiple layers (i.e. a

multi-aquifer system). The dimensions of the multi-aquifer system are assumed to be 32 m in length, 32 m in width, and 20 m in height. It is composed of 7 layers from top to bottom: A coarse sand layer with 3.5 m in thickness (1st layer), a medium sand layer with 2 m in thickness (2nd layer), another coarse sand layer with 3.5 m in thickness (3rd layer), a fine sand layer with 2 m in thickness (4th layer), one more coarse sand layer with 3.5 m in thickness (5th layer), a clay layer with 2 m in thickness (6th layer), and finally a coarse sand layer with 3.5 m in thickness (7th layer), as shown in Figure 5. The well screen starts from $z$=5.5 m to $z$=16.5 m. The well screen is open in layers 2 – 6. The injection or extraction point is located at the top of the well screen. The hydraulic conductivities of the coarse sand (layers 1, 3, 5, and 7), the medium sand (layer 2), the fine sand (layer 4) and the clay (layer 6) are 10 m/day, 0.1 m/day, 0.01 m/day, and 0.001 m/day, respectively. The common factors for all 7 layers are a specific storage of 0.0001 $m^{-1}$, a porosity of 0.3, and a longitudinal dispersivity of 0.5 m.

To set up the numerical simulation, the aquifer is discretized into 40 columns × 40 rows × 7 layers. The horizontal discretization is uniform, e.g. $\Delta x = 0.8$ m, and $\Delta y = 0.8$ m, while the vertical discretization matches the layer thickness.

Figures 6A and 6B show the comparison of BTCs between the previous model and the new models of this study. The injection well is located at the aquifer center with a flow rate of 20 $m^3$/day. Legends of "z=15 m", "z=12.75 m", "z=10 m", and "z=7.25 m" represent the observed locations at 2nd layer (the medium sand layer), 3rd layer (the second coarse sand layer), 4th layer (the fine sand layer), and 5th layer (the third coarse sand layer), respectively, as shown in Figure 5. Figure 6A shows that the solute concentration obtained by the new models is smaller than that by the previous models, implying that the previous models overestimate the solute concentration in the wellbore. This is because Eqs. (8) – (12)

~~underestimate the water volume in the wellbore. Figure 6B shows the comparison of BTCs in the aquifer, and the legends are the same with ones in Figure 6A. One may find that BTCs computed by the new models are lower than BTCs generated by the previous models, and the reason is the same with one in Figure 6A. Additionally, the values of BTCs at $z$=12.75 m and $z$=7.25 m are greater than those at $z$=15 m and $z$=10 m. This is because the locations of $z$=12.75 m and $z$=7.25 m are in the coarse sand layer, whose higher permeability makes solute transport much easier and faster.~~

## 6. Summary and conclusions

Solute transport in a well-aquifer system has attracted the attention of scholars in hydrogeology and environmental science during the past few decades. Due to the complexity of the flow field, numerical modeling has been widely used to study the fate and transport of contaminants ~~tes~~ in the subsurface through the interaction of an open borehole and the surrounding aquifer. By revisiting the previous ~~3D~~ mathematical model of reactive transport in the Cartesian coordinate system, we found that it could not properly describe the wellbore storage in the confined aquifer. In this study, a revised model is developed based on the mass balance principle in a well-confined aquifer system. The conclusions are summarized as follows:

(1) In the early stage of the pumping phase, the volume of water in the wellbore is critical for the wellbore storage of solute transport. Greater volume results in smaller concentration of solute in the wellbore, due to the mixing processes between the original water in the wellbore and water entering the wellbore or leaving the wellbore. (2) A revised ~~3D~~ model of reactive transport is proposed and tested

against the analytical solutions, and it is much better than the previous models in describing the wellbore storage for a well penetrating a confined aquifer.

(~~2~~3) For the injection well test case, the previous models of reactive transport may cause errors, which are considerable in both aquifer and wellbore. ~~For the extraction well test case, such errors are obvious in the wellbore, but not in the aquifer.~~

~~(3) The previous models overestimate the solute concentration in the injection well test case, while underestimate the concentration in the extraction well test case.~~

**Code and data availability:** The code/datasets used and/or ~~analysed~~analyzed during the current study are available from the corresponding author upon reasonable request.

**Author contributions:** Methodology, derivation, code, and formal analysis, writing original draft: YG. Conceptualization, writing original draft, writing-review and editing, and supervision: QW.

**Competing interests:** The contact author has declared that neither they nor their co-authors have any competing interests.

**Acknowledgments**

This research was partially supported by Programs of Natural Science Foundation of China (No. 41972250), and Innovative Research Groups of the National Nature Science Foundation of China (No. 41521001). We would like to thank the editors and two anonymous reviewers for their constructive feedback which helped to improve the article.

## References


Anderson, M. P., Woessner, W. W., and Hunt, R. J.: Applied groundwater modeling: simulation of flow and advective transport, Academic press2015.

Chen, C. S.: Analytical and approximate solutions to radial dispersion from an injection well to a geological unit with simultaneous diffusion Into adjacent strata, Water Resources Research, 21(8), 1069-1076, https://doi.org/10.1029/WR021i008p01069, 1985.

Chen, J.-S., Liu, Y.-H., Liang, C.-P., Liu, C.-W., and Lin, C.-W.: Exact analytical solutions for two-dimensional advection–dispersion equation in cylindrical coordinates subject to third-type inlet boundary condition, Advances in Water Resources, 34(3), 365-374, https://doi.org/10.1016/j.advwatres.2010.12.008, 2011.

Chen, J. S.: Analytical model for fully three-dimensional radial dispersion in a finite-thickness aquifer, Hydrol. Process., 24(7), 934-945, https://doi.org/10.1002/hyp.7541, 2010.

Chen, Y. J., Yeh, H. D., and Chang, K. J.: A mathematical solution and analysis of contaminant transport in a radial two-zone confined aquifer, Journal of Contaminant Hydrology, 138-139(2012), 75-82, https://doi.org/10.1016/j.jconhyd.2012.06.006, 2012.

El-Kadi, A. L.: Applying the USGS Mass-Transport Model (MOC) to Remedial Actions by Recovery Wells, Groundwater, 26(3), 281-288, https://doi.org/10.1111/j.1745-6584.1988.tb00391.x, 1988.

Konikow, L. F. and Grove, D. B.: Derivation of equations describing solute transport in ground water, US Geological Survey, Water Resources Division, https://doi.org/10.3133/wri7719. 1977.

Konikow, L. F. and Hornberger, G. Z.: Use of the multi-node well (MNW) package when simulating solute transport with the MODFLOW ground-water transport process, US Geological Survey Techniques and Methods, 6-A15, https://doi.org/10.3133/tm6A15. 2006.

Konikow, L. F., Hornberger, G. Z., Halford, K. J., and Hanson, R. T.: Revised multi-node well (MNW2) package for MODFLOW ground-water flow model, US Geological Survey Techniques and Methods, 6-A30, https://doi.org/10.3133/tm6A30. 2009.

Novakowski, K. S.: The analysis of tracer experiments conducted in divergent radial flow fields, Water resources research, 28(12), 3215-3225, https://doi.org/10.1029/92WR01722. 1992.

Phanikumar, M. S. and McGuire, J. T.: A multi-species reactive transport model to estimate biogeochemical rates based on single-well push-pull test data, Computers & Geosciences, 36(8), 997-1004, https://doi.org/10.1016/j.cageo.2010.04.001, 2010.

Pruess, K., Oldenburg, C., and Moridis, G.: TOUGH2 User's Guide, 2011.

Schwartz, R., McInnes, K., Juo, A., Wilding, L., and Reddell, D.: Boundary effects on solute transport in finite soil columns, Water Resources Research, 35(3), 671-681, https://doi.org/10.1029/1998WR900080. 1999.

Trefry, M. G. and Muffels, C.: Feflow: A finite-element ground water flow and transport modeling tool, Ground Water, 45(5), 525-528, https://doi.org/10.1111/j.1745-6584.2007.00358.x, 2007.

Veling, E. J. M.: Radial transport in a porous medium with Dirichlet, Neumann and Robin-type inhomogeneous boundary values and general initial data: analytical solution and evaluation, J. Eng. Math., 75(2012), 173-189, https://doi.org/10.1007/s10665-011-9509-x, 2012.

Wang, Q. R. and Zhan, H. B.: Radial reactive solute transport in an aquifer-aquitard system, Advances in Water Resources, 61(2013), 51-61, https://doi.org/10.1016/j.advwatres.2013.08.013, 2013.

Yeh, H. D. and Chang, Y. C.: Recent advances in modeling of well hydraulics, Advances in Water Resources, 51(2013), 27-51, https://doi.org/10.1016/j.advwatres.2012.03.006. 2013.

Zheng, C. and Wang, P. P.: MT3DMS: a modular three-dimensional multispecies transport model for simulation of advection, dispersion, and chemical reactions of contaminants in groundwater systems; documentation and user's guide, Alabama Univ University, http://hdl.handle.net/11681/4734 (last access: 11 May 2023). 1999.

~~Figure Captions~~

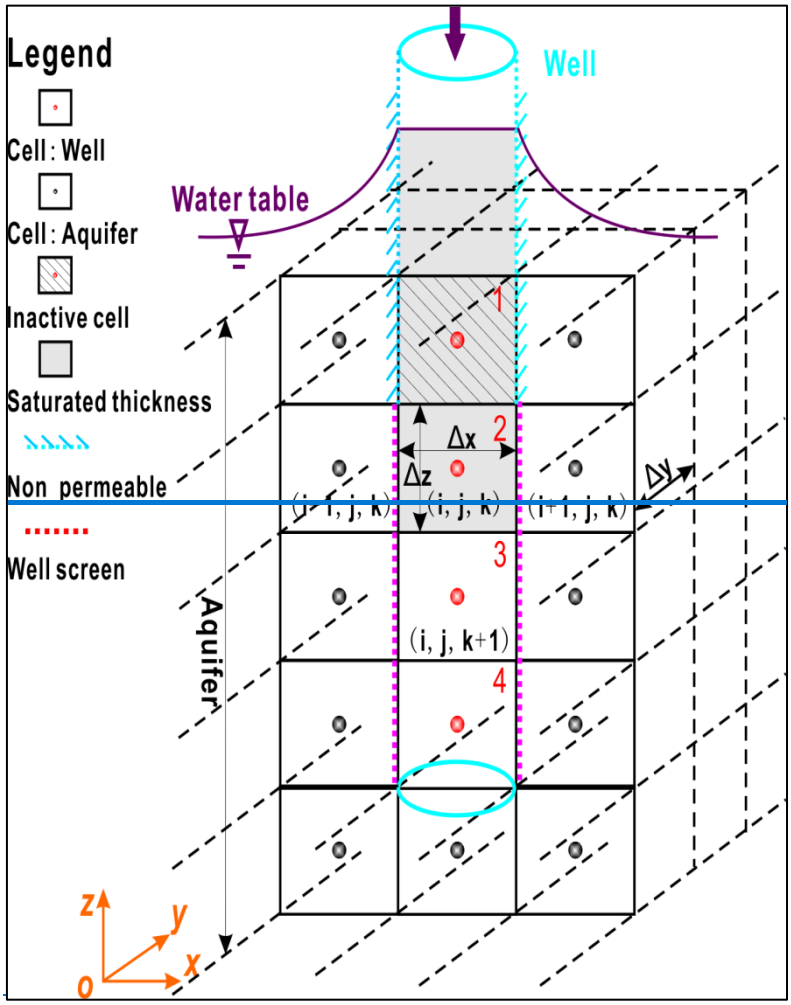


**Figure 1.** ~~Schematic diagram of the grid system in a numerical simulation of a partially penetrating well. Black lines represent the discretization of the aquifer including the wellbore in the aquifer (e.g. Cell 1, Cell 2, Cell 3, and Cell 4). The part of the wellbore located above the aquifer is not included in the grid system.~~

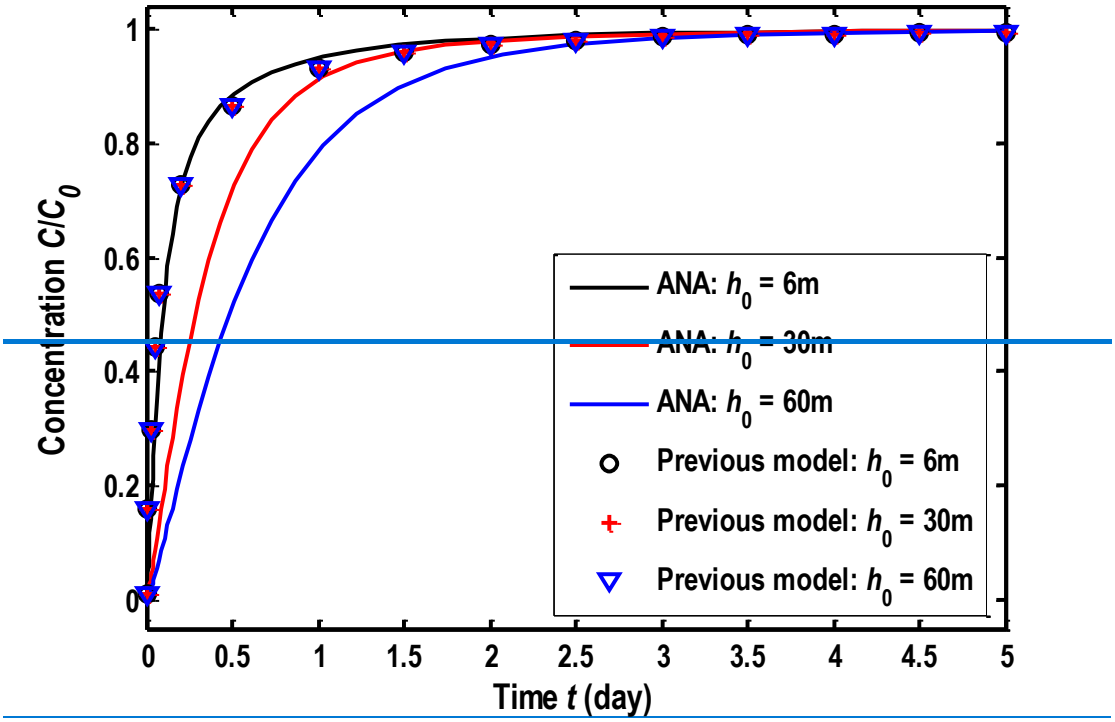


(a) Numerical solutions computed by the previous model

**Figure 2.** Comparison between BTCs based on analytical and numerical methods in the wellbore under steady state flow conditions. ANA: Analytical solutions.

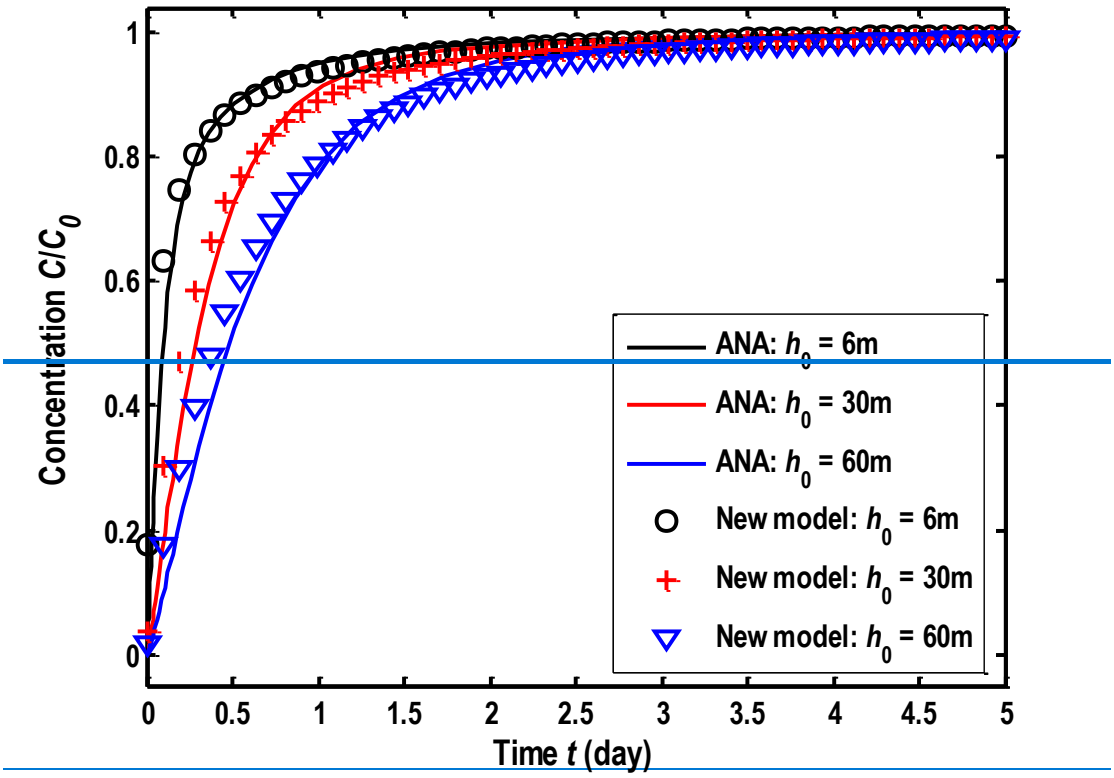


480 ~~(b) Numerical solutions computed by the revised new model~~

**~~Figure 2.~~** ~~Comparison between BTCs based on analytical and numerical methods in the wellbore under steady state flow conditions. ANA: Analytical solutions.~~

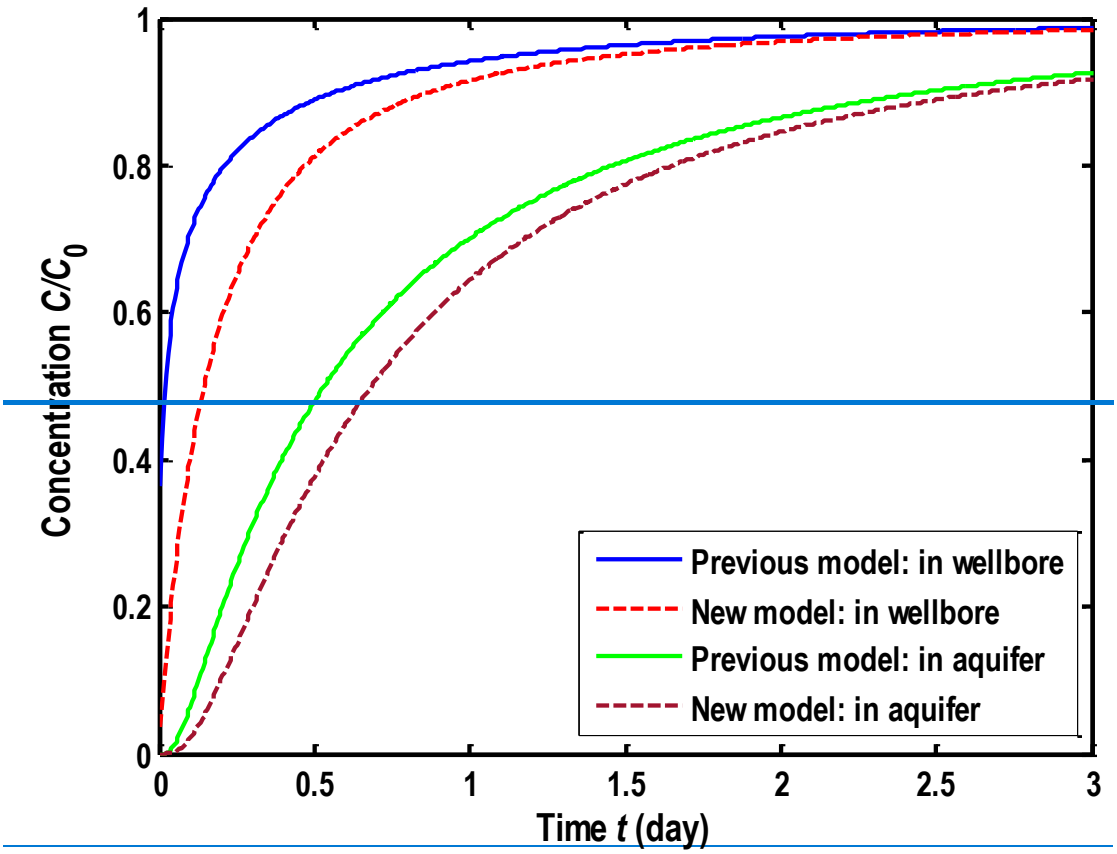


485 **~~Figure 3.~~** ~~Comparison of BTCs for the injection well test.~~

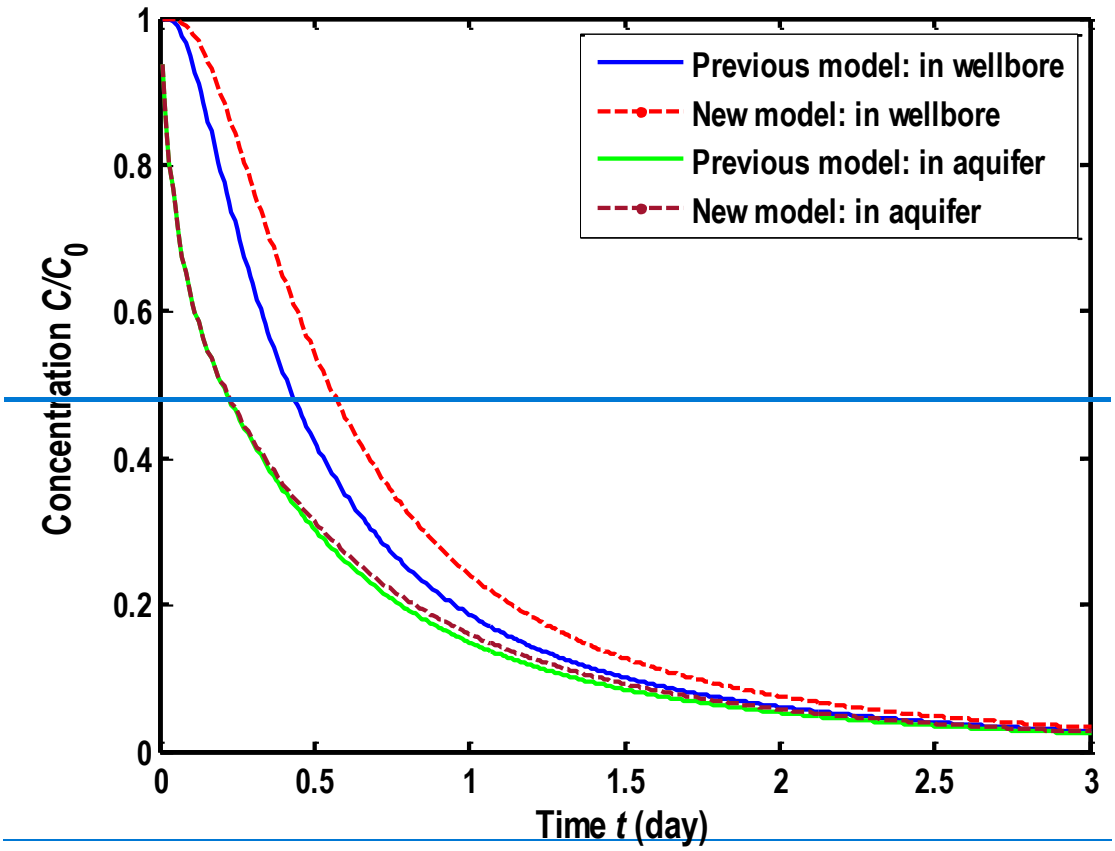


**Figure 4.** Comparison of BTCs for the extraction well test.

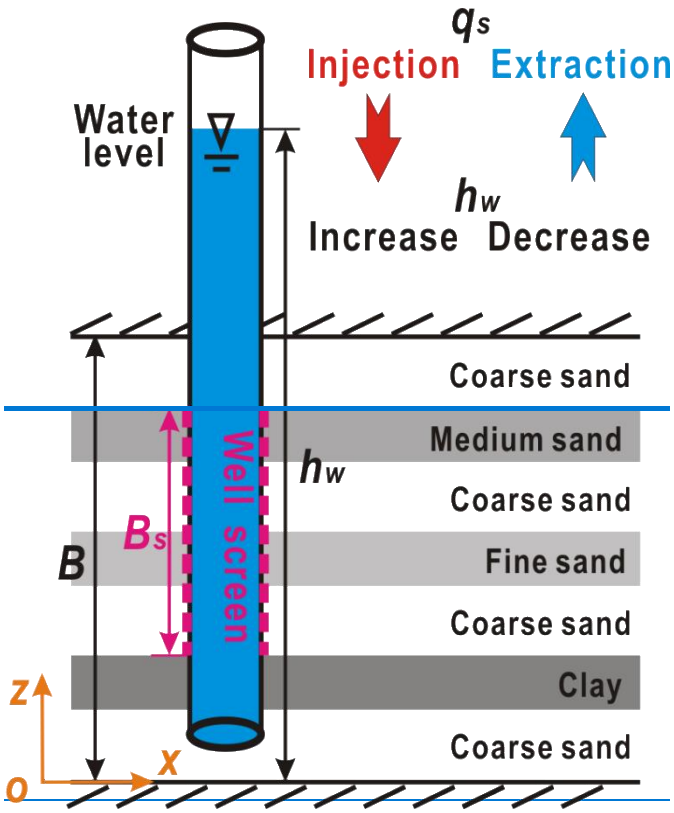


**Figure 5.** Schematic diagram of the well-aquifer system. The well partially penetrates the stratified aquifer.

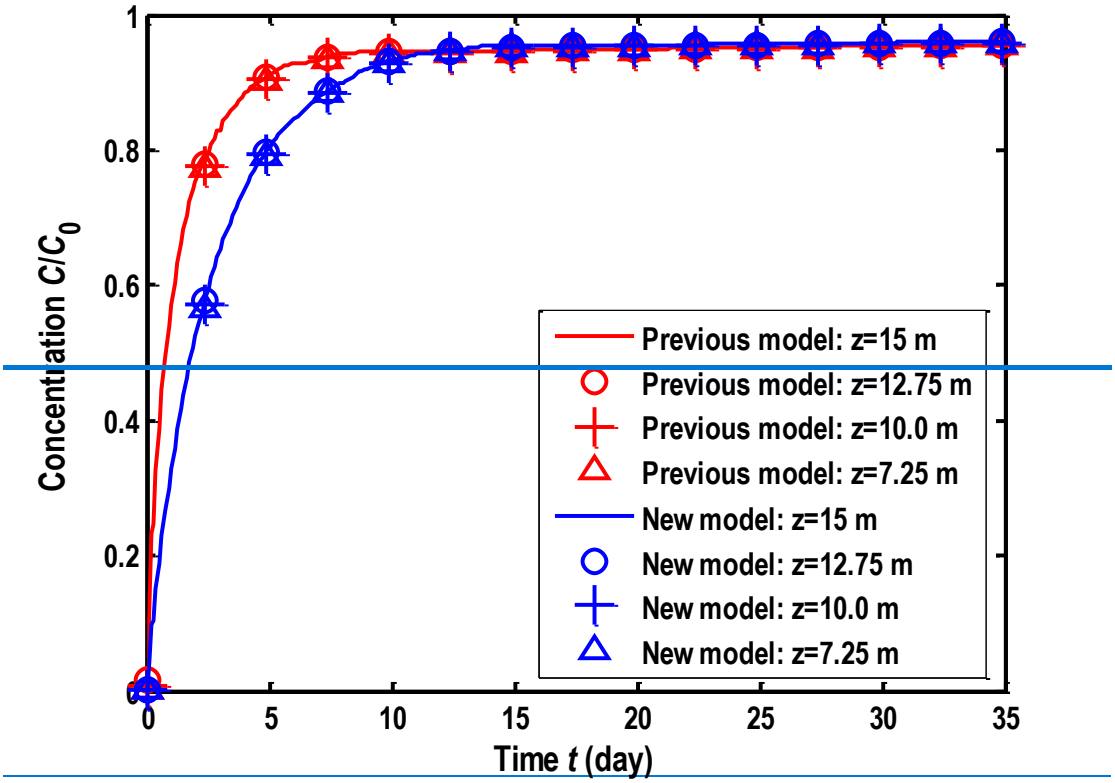


~~(a) BTC in the wellbore~~

**~~Figure 6.~~** ~~Comparison of BTCs for the two-well test under transient flow conditions.~~

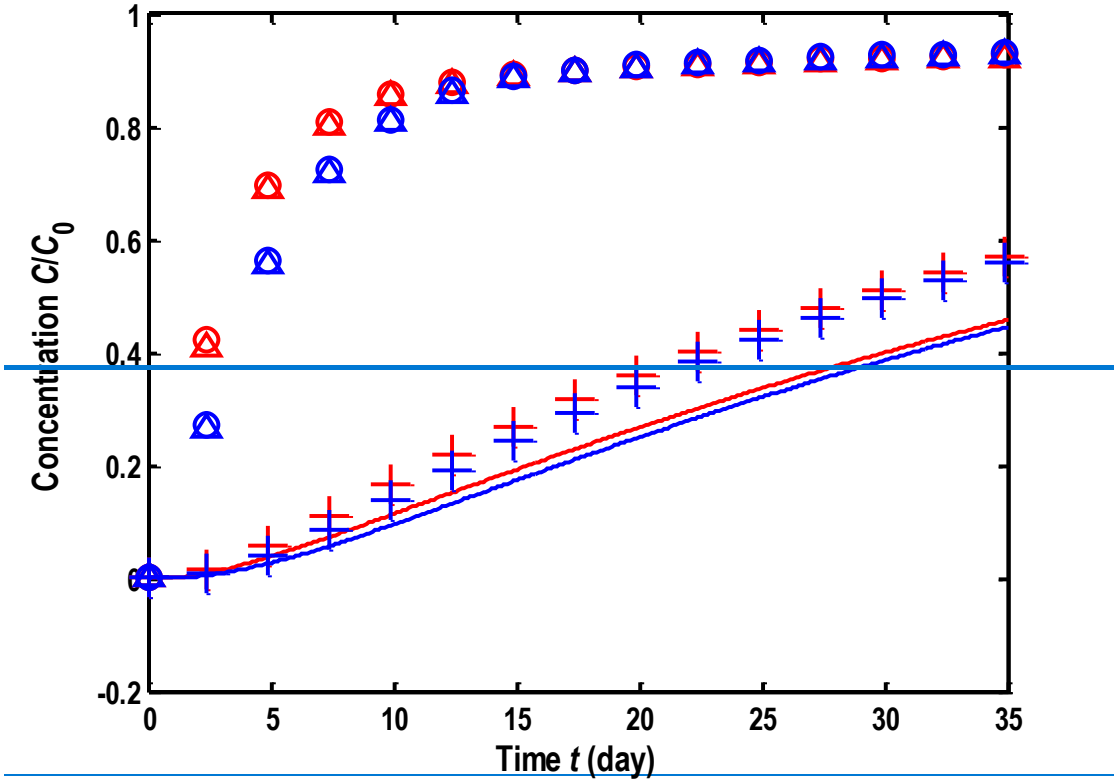


(b) BTC in the aquifer, 1.2 m away from well.

**Figure 6.** Comparison of BTCs for the two-well test under transient flow conditions.